DALTON

Zinc(II) N_2S_2 Schiff-base complexes incorporating pyrazole: syntheses, characterization, tautomeric equilibria and racemization kinetics†

Oren P. Anderson,[a] Agnete la Cour,*[,b] Matthias Findeisen,[c] Lothar Hennig,[d] Ole Simonsen,[b] Lucille F. Taylor[a] and Hans Toftlund[b]

[a] *Department of Chemistry, Colorado State University, Fort Collins, Colorado 80523, USA*
[b] *Department of Chemistry, Odense University, DK-5230 Odense M, Denmark*
[c] *Department of Analytical Chemistry, Leipzig University, D-04103 Leipzig, Germany*
[d] *Department of Organic Chemistry, Leipzig University, D-04103 Leipzig, Germany*

Chiral four-co-ordinate zinc(II) N_2S_2 complexes with bi- or tetra-dentate Schiff-base ligands have been prepared and their properties investigated by spectroscopic methods. The single-crystal structures have been determined for two different crystalline modifications of bis[4-(2,6-dimethylphenyliminomethyl)-1-methyl-3-phenylpyrazole-5-thiolato-*N*,*S*]zinc(II) **1**, a triclinic modification (**1a**) and an orthorhombic one (**1b**), and for bis(4-isopropyliminomethyl-3-methyl-1-phenylpyrazole-5-thiolato-*N*,*S*)zinc(II) **2**. The co-ordination geometry of **1** is similar to that found for the active site of horse liver alcohol dehydrogenase. The asymmetric units in the structures of **1** contain two pseudo-tetrahedral complexes slightly distorted towards *trans*-planar co-ordination geometries; the angles θ between the N–Zn–S and S′–Zn–N′ planes are 97.0 and 96.8 (modification **1a**), 92.5 and 98.6 ° (**1b**) for the two molecules, respectively. The structure of **2** also reveals a pseudo-tetrahedral geometry and a slight distortion towards a *cis*-planar co-ordination (θ = 82.63°) typical of $M^{II}N_2S_2$ complexes. The racemization kinetics for the process $\Delta \rightleftharpoons \Lambda$ have been investigated for four complexes by temperature-dependent ^{1}H NMR spectroscopy and the activation parameters derived for complexes **1** [$\Delta H^{\ddagger} = 80.7$ kJ mol^{-1}, $\Delta S^{\ddagger} = -2.9$ J K^{-1} mol^{-1}, $\Delta G^{\ddagger}$ (25 °C) = 81.6 kJ mol^{-1}] and **2** [$\Delta H^{\ddagger} = 67.2$ kJ mol^{-1}, $\Delta S^{\ddagger} = -57.8$ J K^{-1} mol^{-1}, $\Delta G^{\ddagger}$ (25 °C) = 84.4 kJ mol^{-1}]. The complexes carrying tetradentate ligands do not racemize below 90 °C. The tautomeric equilibria for the protonated pro-ligands and the preferred mesomer of the complexes have been investigated by NMR and UV spectroscopy. The pro-ligands are mainly in the thione form, while the ligands are thiolate-like when co-ordinated to zinc(II). The evolution of the electronic spectra with time, however, reveals the development of thiol- or thiolate-like forms for both pro-ligands and complexes.

Zinc in biological systems is invariably in the oxidation state II and acts predominantly as a Lewis acid. About 20 zinc enzymes are known, and most are involved in hydrolysis reactions.[1] In these systems zinc is typically four-co-ordinate and ligated by hard donors (N or O). The co-ordination geometry is pseudo-tetrahedral.

The only well characterized zinc enzyme involved in redox chemistry is the alcohol dehydrogenase which reversibly catalyses the oxidation of primary and secondary alcohols to aldehydes and ketones, equation (1) (NADH = reduced

$$RR'CHOH + NAD^+ \rightleftharpoons RR'C{=}O + NADH + H^+ \quad (1)$$

nicotinamide adenine dinucleotide). The first crystal structure of alcohol dehydrogenase isolated from horse liver (HLADH) was published 20 years ago.[2] The enzyme is a dimer, and each subunit contains two zinc atoms in pseudo-tetrahedral geometries. One zinc atom is ligated by cysteinate through S alone and is thought to play a structural function. The catalytically active zinc atom is ligated by one histidine residue and two negatively charged cysteinate groups (see Scheme 1).

We have synthesized five new zinc(II) N_2S_2 Schiff-base complexes. The single-crystal structures have been determined for **1** and **2** and may be compared with that of the active site of HLADH. The electrochemical properties of **1** and of its pro-ligand have been studied, together with the structural changes with time and the stereochemical changes with temperature in solution.

† *Supplementary data available* (No. SUP 57186, 3 pp.): rate constants and electronic spectral data. See Instructions for Authors, *J. Chem. Soc., Dalton Trans.*, 1997, Issue 1.

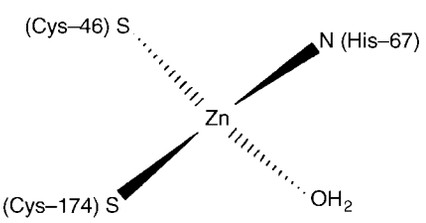

Scheme 1 The active site of HLADH. The water molecule is replaced by a substrate in catalytic cycles

Results and Discussion

Yields and analytical data are presented in Table 1.

Crystal structures of complexes 1 and 2

Selected bond lengths and angles are given in Tables 2 and 4 (complex **1**) and in Table 3 (complex **2**); the molecular structures are shown in Figs. 1–3.

Complex **1** crystallizes as a racemate. The structures of two crystalline modifications [one centrosymmetric and triclinic, **1a**, see Fig. 1, and one non-centrosymmetric and orthorhombic, **1b**, see Fig. 2(*a*) and (*b*)] were determined. The asymmetric units in both structures contain two zinc(II) complexes and either two (**1a**) or one (**1b**) molecule(s) of acetonitrile. In the case of modification **1b** large standard deviations of the parameters and some difficulty in correct localization of the atoms of the phenyl groups, especially C(20A) and C(32), resulting in bond lengths of 1.48(3) and 1.29(3) Å for C(20A)–C(25A) and C(32)–C(33), respectively, are ascribed to weak reflections and a data set of relatively low resolution (see Experimental section).

As solved and refined in the non-centrosymmetric space group $Pc2_1n$ (see Experimental section) the asymmetric unit in the structure of modification **1b** contains two zinc(II) complexes. Plots of the complexes in the asymmetric unit [Fig. 2(*b*)] showed that these might be related by an inversion centre, and translation of the origin to the pseudo-inversion centre followed by pairwise comparison of the coordinates for the atoms of one complex with the corresponding atoms of the other reveals rather close $xyz/-x-y-z$ correlation. The largest deviation from this symmetry is 0.9 Å. However, several attempts to solve and refine the structure in the centrosymmetric space group *Pcmn* by an integrated Patterson and direct method procedure (see Experimental section) using the known structure as a model were unsuccessful; about one quarter of

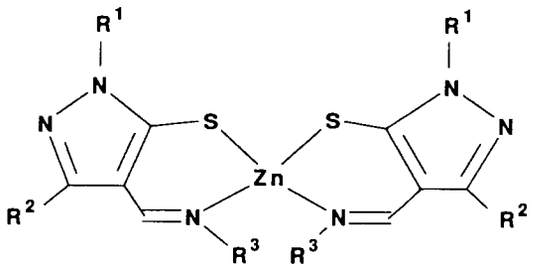

1 R^1 = Me, R^2 = Ph, R^3 = $C_6H_3Me_2$-2,6

2 R^1 = Ph, R^2 = Me, R^3 = Pr^i

3 R^1 = Me, R^2 = Ph, R^3 = Pr^i

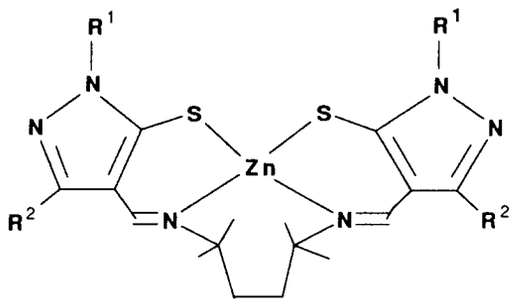

4 R^1 = R^2 = Me

5 R^1 = Ph, R^2 = Me

Table 1 Analytical data for the complexes[a]

Complex	Yield[b] (%)	Analysis (%)[c] C	H	N	EI mass spectrum, *m/z*[d]
1	82	63.7 (64.6)	5.00 (5.15)	11.75 (11.9)	703
2	58	57.05 (57.75)	5.45 (5.55)	14.3 (14.45)	580
4	87	49.3 (49.65)	6.15 (6.25)	17.5 (17.35)	482
5	58	59.2 (59.25)	5.70 (5.65)	13.95 (13.8)	606

[a] Data for complex **3** were presented in ref. 3(*b*); **4** was recrystallized from EtOH–CH_2Cl, **1**, **2** and **5** were not recrystallized. [b] From ligand. [c] Calculated values in parentheses. [d] The molecular ion, M^+.

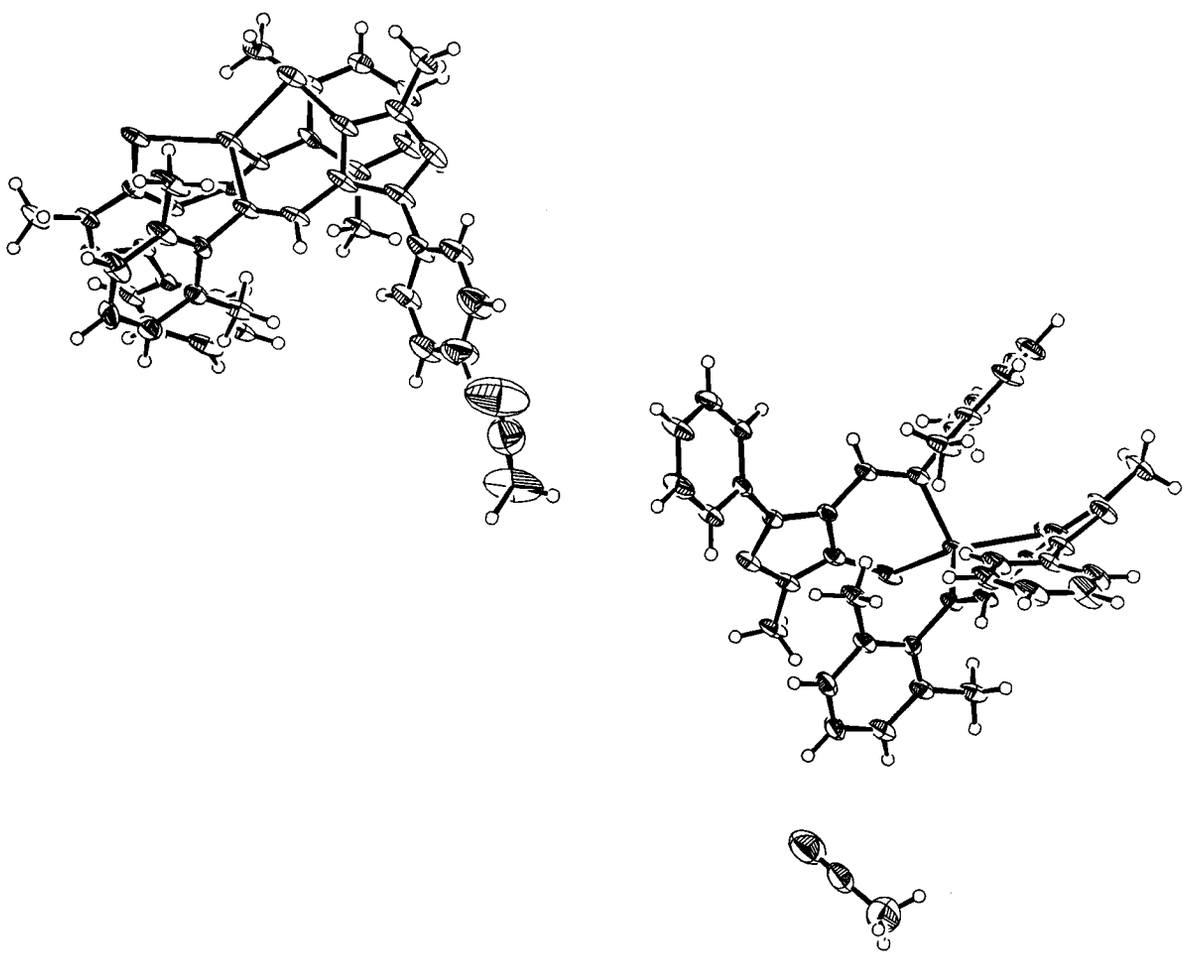

Fig. 1 Asymmetric unit of the triclinic modification **1a** of complex **1** with 50% probability thermal ellipsoids for non-hydrogen atoms [numbering as in Fig. 2(*a*)]

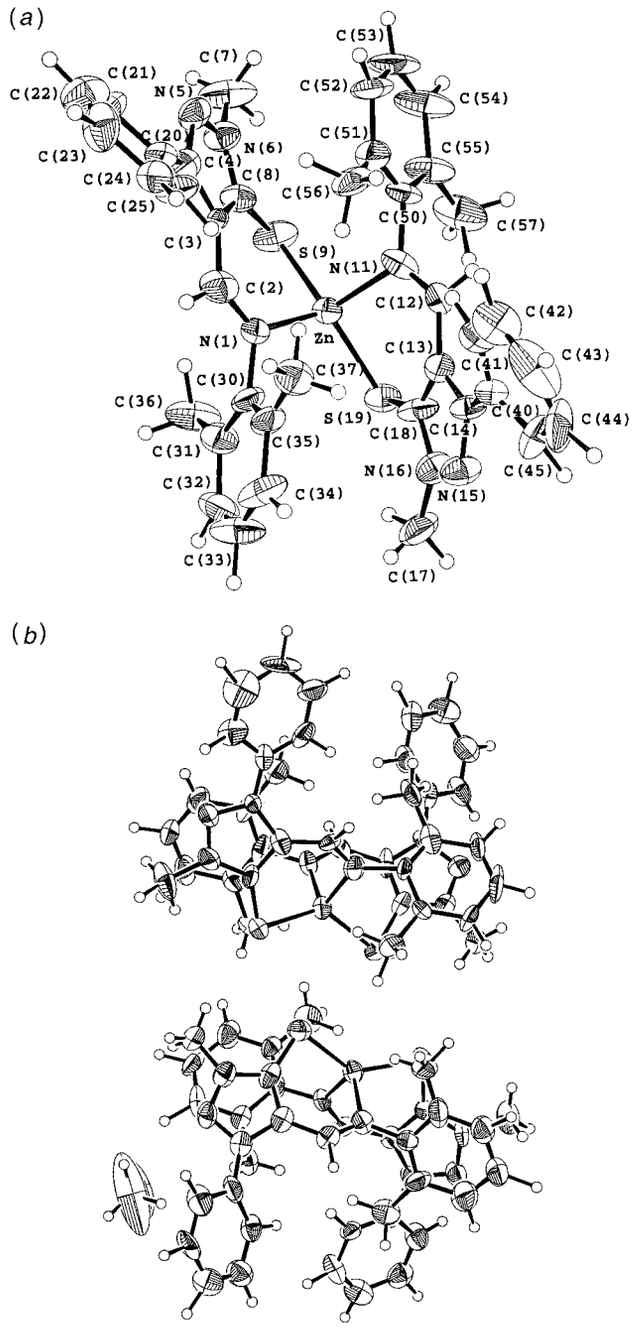

Fig. 2 Molecular structure (*a*) and the asymmetric unit (*b*) for the orthorhombic modification **1b** of complex **1**, with 50% probability thermal ellipsoids for non-hydrogen atoms

the complex could be located, but refinement of the fragment was not possible. Attempts to resolve the structure by direct methods in *Pcmn* were also without result. The *E* statistics indicate that a significant portion of the structure appears to be centrosymmetric, but that the rest is not: theoretical values for the mean values of $|E|$, $|E^2 - 1|$ and $|E^2 - 1|^2$ for a centrosymmetric structure are 0.798, 0.968 and 2.000, respectively; for a non-centrosymmetric structure the values are 0.886, 0.736 and 1.000. The corresponding values for the structure of modification **1b** are 0.809, 0.866 and 1.442. Overall, the non-centrosymmetric model for the structure of **1b** provides the best description that is available.

Several intermolecular distances in the structures of complex **1** are close to the sums of the van der Waals radii (3.2 Å for Zn···S, 3.6 Å for S···S),[5a] see Table 2. Possibly the lack of an intramolecular S···S contact often seen in metal-free systems[5b–d] and in N_2S_2 Schiff-base complexes[6a] is compensated

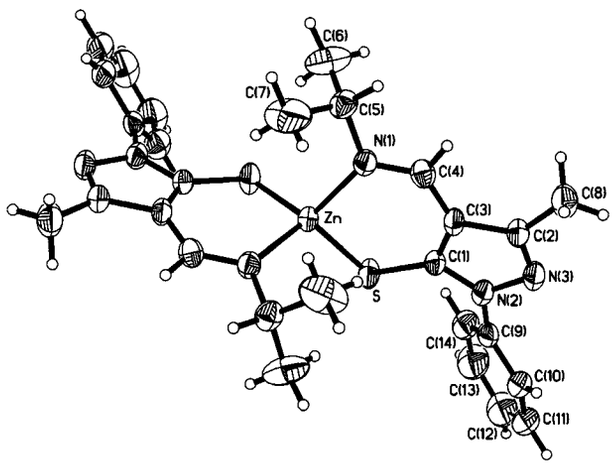

Fig. 3 Molecular structure of complex **2**, with 50% probability thermal ellipsoids for non-hydrogen atoms

for by intermolecular interactions forming a weakly bound dimer of the complex. In the triclinic and centrosymmetric structure **1a** each of the molecules of the asymmetric unit is passed across an inversion centre to give the entire unit-cell contents. The results of one of the inversions gives an inverted molecule which interacts with the original one (molecule **A**), while the other gives an inverted molecule that does not interact with the original one. In the orthorhombic structure **1b** every molecule is involved in interactions, *i.e.* with the other molecule of the asymmetric unit. The differences observed between **1a** and **1b** are ascribed to the different speed of crystallization; 4–5 d for **1a**, more than 2 weeks for **1b**, see Experimental section.

Crystals of complex **2** contain a single enantiomer. The molecules (Fig. 3) exhibit crystallographically imposed C_2 symmetry with the crystallographic two-fold axis running through the Zn atom and bisecting the N–Zn–N′ and S–Zn–S′ angles. The structure contains discrete molecules without any special intermolecular interactions.

The Zn–N and Zn–S distances in the three structures are as expected.[6,7] The C–S bonds are of intermediate length between that of a thione and that of a thiol (C–C=S 1.6, C–C–SH 1.8 Å)[8] which is normal for N_2S_2 Schiff-base complexes.[6] The bond lengths in the chelate rings support the expected delocalization of electron density in all three complexes.

The co-ordination geometry of complex **2** is typical of four-co-ordinate zinc(II) complexes.[6,7] The angles centred on Zn fall within the normal range, and the angle θ between the N–Zn–S planes is close to the ideal for a tetrahedron (90°), as expected for a four-co-ordinate d^{10} ion such as Zn^{II}. In contrast with the slight distortion towards a *cis*-planar geometry seen in **2** [θ = 82.63(8)°] followed by a small S–Zn–S′ angle [103.05(6)°] and a relatively short intramolecular S···S′ distance [3.590(2) Å], the distortion in **1** is towards a *trans*-planar geometry* [θ 97.0(2) and 96.8(2) (**1a**), 92.5(5) and 98.6(4)° (**1b**)]. This results in large S(9)–Zn–S(19) angles [130.98(5) and 136.42(5) (**1a**), 131.3(2) and 137.4(2)° (**1b**)] and intramolecular S···S distances significantly greater than the van der Waals contact distance [4.144(2) and 4.241(2) (**1a**), 4.152(7) and 4.286(7) Å (**1b**)]. The 2,6-xylyl substituents, approximately orthogonal to the plane of the chelate rings (see Table 2), may be responsible for the *trans* distortion of **1**. Bis(bidentate ligand)nickel(II) N_2S_2 complexes incorporating pyrazole are normally pseudo-tetrahedral and *cis*-distorted;[6a] however, a 2,6-xylyl-substituted nickel(II) complex similar to **1** has an unusual *trans*-

* A complex is defined as *cis* if the angle θ between the normals to the planes N–M–S and S′–M–N′ is <90°, *trans* if θ > 90°, M being the origin of a Carthesian coordinate system and N, S, S′ and N′ vectors in this coordinate system.

Table 2 Selected geometrical parameters for complex **1** (see also Table 4)

Selected intermolecular distances (Å)

Triclinic **1a**		Orthorhombic **1b**	
S(9A)···S(9A′)	3.308(2)	S(9)···S(9A)	3.265(6)
S(9A)···S(19A′)	3.702(2)	S(9)···S(19A)	3.866(6)
Zn···S(9A′)	3.640(2)	S(19)···S(9A)	3.669(6)
		Zn···S(9A)	3.696(4)
		S(9)···Zn(A)	3.687(4)

Selected bond lengths (Å) and angles (°)

	Triclinic **1a**		Orthorhombic **1b**	
	1	**1A**	**1**	**1A**
N(1)–C(2)	1.296(5)	1.298(6)	1.27(2)	1.28(2)
C(2)–C(3)	1.430(6)	1.428(6)	1.47(2)	1.45(2)
C(3)–C(8)	1.410(6)	1.415(6)	1.35(2)	1.39(2)
C(8)–S(9)	1.733(5)	1.739(4)	1.76(2)	1.71(2)
N(11)–C(12)	1.293(6)	1.295(6)	1.30(2)	1.30(2)
C(12)–C(13)	1.428(6)	1.430(6)	1.43(2)	1.46(2)
C(13)–C(18)	1.412(7)	1.415(6)	1.41(2)	1.41(2)
C(18)–S(19)	1.730(5)	1.740(4)	1.68(2)	1.70(2)
Zn–N(1)–C(2)	122.2(3)	121.8(3)	121(1)	120(1)
N(1)–C(2)–C(3)	124.0(4)	124.6(4)	125(1)	127(1)
C(2)–C(3)–C(8)	129.2(4)	128.1(4)	126(1)	126(1)
C(3)–C(8)–S(9)	132.8(3)	132.5(3)	133(1)	134(1)
Zn–S(9)–C(8)	94.8(2)	95.3(2)	94.3(5)	95.2(6)
Zn–N(11)–C(12)	121.5(3)	122.3(3)	120(1)	122(1)
N(11)–C(12)–C(13)	124.3(5)	124.4(4)	124(1)	124(1)
C(12)–C(13)–C(18)	129.8(5)	127.3(4)	128(1)	126(1)
C(13)–C(18)–S(19)	132.7(4)	133.1(3)	134(1)	134(1)
Zn–S(19)–C(18)	94.2(2)	94.4(2)	95.3(5)	94.8(5)
The angle θ/°				
S(9)–Zn–N(1) / N(11)–Zn–S(19)	97.0(2)	96.8(2)	92.5(5)	98.6(4)
Selected torsion angles (°)				
Zn–N(1)–C(30)–C(31)	−80.6(5)	73.3(6)	−76.8(7)	76.8(8)
C(2)–N(1)–C(30)–C(31)	93.6(6)	−105.4(6)	106(1)	−103(1)
Zn–N(11)–C(50)–C(51)	95.8(5)	−102.7(6)	91.7(7)	−101.1 6
C(12)–N(11)–C(50)–C(51)	−87.3(6)	76.6(7)	−86(1)	85(1)

Estimated standard deviations (e.s.d.s) of the least significant digits are given in parentheses.

Table 3 Selected bond distances (Å) and angles (°) for complex **2**

Zn–N(1)	2.039(3)	C(4)–C(3)	1.415(5)
Zn–S	2.293(1)	C(3)–C(1)	1.408(5)
N(1)–C(4)	1.306(5)	C(1)–S	1.719(4)
S···S′	3.590(2)		
N(1)–Zn–S	103.20(9)	S–C(1)–C(3)	130.9(3)
N(1)–Zn–N(1′)	113.0(2)	C(1)–C(3)–C(4)	131.1(3)
N(1)–Zn–S′	117.27(9)	C(3)–C(4)–N(1)	128.1(3)
S–Zn–S′	103.05(6)	Zn–N(1)–C(4)	121.9(3)
Zn–S–C(1)	101.0(1)	N(1)–Zn–S / S′–Zn–N(1′)	82.63(8)*

E.s.d.s of the least significant digits are listed in parentheses. * The angle θ.

planar co-ordination geometry in the solid state (θ = 180°).[9a] Further, the bis(bidentate ligand)nickel(II) N_2O_2 Schiff-base complexes of the salicylaldimine type having *o*-methylphenyl-substituted donor nitrogen atoms are diamagnetic, suggestive of a planar co-ordination geometry, in the solid state and in solution in contrast with the analogous *m*- and *p*-methylphenyl-substituted complexes.[9b] As ligand-field considerations are not appropriate for Zn^{II} we must ascribe the *trans* distortion of the complexes **1** to anisotropic crystal-packing forces.

The co-ordination sphere of complex **1** is similar to that of the Zn atom at the active site of HLADH[4] (see Table 4).

Electrochemistry

The resemblance of complex **1** to the active site of HLADH inspired us to investigate the influence of the Zn atom on the electrochemistry of the ligand. One imine function is assumed to be a substituent of the oxidized substrate, see equation (1) and Scheme 1. The results are shown in Fig. 4. The partly quasi-reversible electrochemical processes are slow. The oxidation of the protonated pro-ligand, curve a, is shifted to a more positive potential, a′, on co-ordination to Zn^{II}. One more oxidation wave, c′, is seen for the complex. Two reduction waves b and d (d not shown) are seen for the pro-ligand. The potential of b′ and probably d′ also becomes more negative for the complex. The wave, c′, may be assigned to oxidation of the thiolate functions of disulfide.[10a] As the experimental conditions were not fully anaerobic, a and a′ can possibly be assigned to oxidation of the thiolate (thiol) functions to SO_2[10b] or of the naked pyrazole nitrogen to *N*-oxide. The reduction of the Schiff base *N*,*N*′-bis(salicylidene)ethane-1,2-diamine (H_2salen)[10c] and the corresponding Bu^tS-protected thio derivative[10d] to the corresponding protonated dihydro- or tetrahydro-compounds takes place under fairly mild conditions. For that reason we assign the reduction waves to reduction of the imine functions. The reduction potential of the imine function does not become more positive upon co-ordination to Zn^{II}. Probably the co-ordination environments formed by the bidentate Schiff-base ligands are

Table 4 The co-ordination geometry (distances in Å, angles in °) of complex **1** compared with that of the active site of horse liver alcohol dehydrogenase

			Triclinic **1a**		Orthorhombic **1b**	
	HLADH[4]		**1**	**1A**	**1**	**1A**
S (Cys-174)–Zn–S (Cys-46)	126(5)	S(9)–Zn–S(19)	130.98(5)	136.42(5)	131.3(2)	137.4(2)
S (Cys-174)–Zn–N (His-67)	105(5)	S(9)–Zn–N(1)	101.8(1)	99.8(1)	98.4(3)	99.1(4)
S (Cys-174)–Zn–O (H_2O)	100(5)	S(19)–Zn–N(11)	102.8(1)	98.6(1)	98.3(4)	96.9(3)
S (Cys-46)–Zn–N (His-67)	112(5)	S(19)–Zn–N(1)	105.0(1)	107.1(1)	112.3(3)	106.1(4)
S (Cys-46)–Zn–O (H_2O)	108(5)	S(9)–Zn–N(11)	107.4(1)	106.3(1)	109.5(4)	107.2(3)
N (His-67)–Zn–O (H_2O)	101(5)	N(1)–Zn–N(11)	107.3(1)	105.9(1)	104.8(5)	108.1(4)
Zn–S	2.3[1c]	Zn–S(9)	2.280(1)	2.285(1)	2.291(5)	2.277(5)
		Zn–S(19)	2.275(2)	2.282(2)	2.266(5)	2.323(5)
Zn–N	2.1[1c]	Zn–N(1)	2.052(4)	2.073(4)	2.03(1)	2.06(1)
		Zn–N(11)	2.070(4)	2.078(4)	2.13(1)	2.09(1)
S···S	4.1	S(9)···S(19)	4.144(2)	4.241(2)	4.152(7)	4.286(7)

E.s.d.s of the least significant digits are given in parentheses.

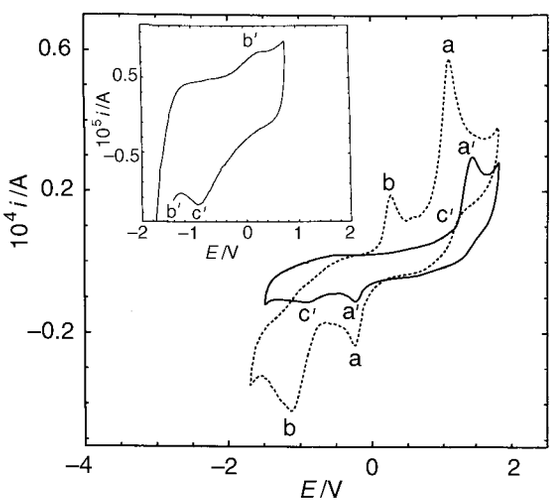

Fig. 4 Cyclic voltammograms for complex **1** (——) and for its pro-ligand (– – –) in MeCN *vs.* Ag–AgCl as reference electrode. Sweep rate: 0.500 V s^{-1}. E_{ox}, E_{red}/V, $E_{1/2}$/V (data for **1** in parentheses): oxidation waves; a (a′) 1.11, −0.25 (1.42, −0.22), 0.43 (0.60); (c′) (≈1.2, −0.88), (≈0.16); reduction waves; b (b′) 0.28, −1.12 (0.32, <−1.4), −0.42 (<−1.08); d (d′), −0.68, −1.48 (−0.51, <−1.4), −1.08 (<−0.96); d and d′ are not shown

far too rigid to create a suitable model for the active site of the HLADH apoenzyme.

NMR spectra

The 200 MHz ^{1}H NMR spectra of complexes **1**, **2** and **5** and assignments are shown in Fig. 5 and the data for **4** are listed in Table 5. The spectra show that complexes **1**, **2** and **4** are pseudo-tetrahedral. The chemical shifts of diastereotopic protons and carbon atoms indicate that the molecules possess C_2 symmetry in solution. Signals from a molecule of C_2 symmetry, *, are observed for **5**. However, a more stable molecule, ○, of lower symmetry, but of the same composition (according to the elemental analyses) exists in a higher concentration. The spectrum of **5** does not change significantly at elevated temperatures (up to 90 °C).

As we were not able to obtain crystals suitable for crystal structure determinations of the complexes with tetradentate ligands (**4** and **5**), nuclear Overhauser effect spectroscopy (NOESY) experiments were performed for **4**. Effects are observed between $H^{3,4}$ and H^6, and between $H^{3,4}$ and H^{10}, but not between $H^{3,4}$ and H^1, *e.g.* indicating a H···H distance > about 2.9 Å[5a] for the latter, and, as evaluated from metal chelate scale models, probably a slight distortion towards a *cis*-planar co-ordination geometry.

It is found with few exceptions that protonated Schiff bases are thione-like both in the solid state and in solution,[6a,11] see II in Scheme 2, and that the preferred mesomers for the corresponding metal chelates are thiolate-like,[11b,c] see III in Scheme 3. The NMR data for the compounds investigated are in accordance with those findings. The spectra of the pro-ligands (shown in part for complex **5**, Fig. 5) indicate that they exist mainly as the thioketo tautomers; the enolic proton observed at δ 13.04 for complex **5** and the aldimine proton at δ 7.76 are coupled (J = 13.8 Hz). Comparison of the ^{13}C NMR spectra for C[7] for the pro-ligands (δ ≈ 170) and the zinc(II) complexes (δ ≈ 160; for the two forms of **5**, δ 158.27 and 162.48) shows the change from a mainly thione to a more thiolate-like form.[11] The spectra of rather concentrated solutions (mmol dm^{-3}) did not change significantly with time (>1 week) in contrast with the electronic spectra of dilute (μmol dm^{-3}) solutions (see below).

Racemization kinetics (see SUP 57186)

The kinetics for the racemization process (2) were evaluated

$$\Delta \rightleftharpoons \Lambda \qquad (2)$$

from the temperature-dependent ^{1}H NMR spectra of diastereotopic indicator protons (see Fig. 6 for complexes **1**, **2** and **4**). The protons of groups Me^3 and Me^4 were used as indicators in all cases. The complexes carrying tetradentate ligands, **4** and **5**, do not racemize, as indicated by Δν and by the absence of any line broadening in the temperature range (25–90 °C) investigated. The slight increase in Δν with temperature for **4** may be attributed to a conformational change towards a more tetrahedral co-ordination geometry. In comparison with the configurational rigidity observed for **4** and **5**, the racemization process is evident in the spectra of the bis(bidentate ligand) complexes, measured from −30 to 130 °C in $CDCl_2CDCl_2$ (**1** and **2**) or from 25 to 130 °C in $C_6D_5NO_2$ (**1**). Metal chelate scale models for complex **1** show that the xylyl ring is not free to rotate either in the planar or in the pseudo-tetrahedral configuration in accordance with experimental results obtained for bis(β-aminothionato)metal(II) complexes (M = Zn or Cd) with 2,4,6-trimethylphenyl-substituted nitrogen donor atoms.[12a] Consequently the temperature dependence for Δν has to be associated with a racemization process and not with a rotation of the xylyl group about the N–C bond.

Rate constants were calculated using equations (3)–(5) (see Experimental section). Corrections were made for the natural temperature dependence for $\Delta\nu^0$ evident in Fig. 6; $\Delta\nu^0$ was extrapolated linearly from plots of Δν *vs.* T in the range 43–71 °C (correlation −0.9996) for complex **1** in $C_6D_5NO_2$, 71–98 °C (correlation −0.9995) for **1** in $CDCl_2CDCl_2$, and 61–89 °C (correlation −0.9995) for **2** in $CDCl_2CDCl_2$. The

Table 5 The NMR data for complex **4** in $CDCl_2CDCl_2$

	1	2	3	4	5	6	7	8	9	10
^{13}C [a]	35.39	11.59	30.85	25.97	37.57	60.66	158.5	148.2	113.2	150.1
^{1}H [a]	3.71	2.26	1.32	1.39	—	1.80, 2.05	—	—	—	8.13
^{1}H [b]	3.71	2.26	1.33	1.42	—	1.82, 2.12	—	—	—	8.16
$\Delta\nu^{a,c}$/Hz			15.40			50.0				
$\Delta\nu^{b,c}$/Hz			17.50			60.0				

Chemical shifts δ are in ppm. [a] At 25 °C. [b] At 90 °C. [c] Proton spectra were measured at 200 MHz.

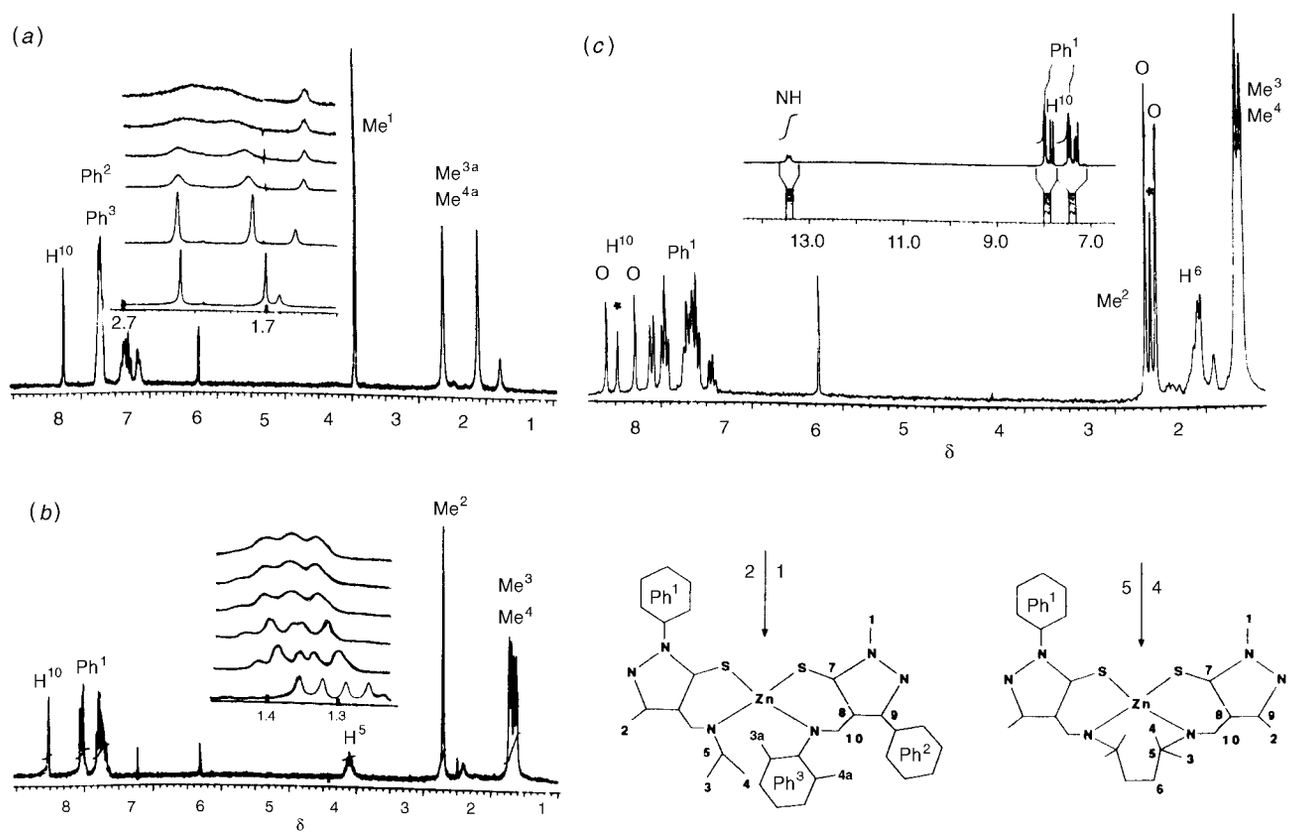

Fig. 5 The 200 MHz ^{1}H NMR spectra of complexes **1** (*a*), **2** (*b*) and **5** (*c*) in $CDCl_2CDCl_2$ and of the pro-ligand H_2L in $CDCl_3$ (inset) at 25 °C. Temperatures for the selected temperature-dependent spectra for complexes **1** and **2** are (from bottom to top) 25, 80, 105, 115, 125 and 130 °C (same scale)

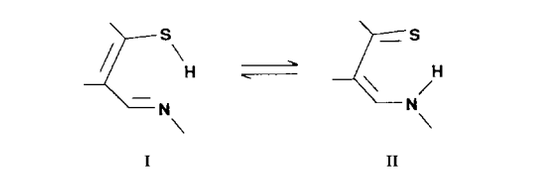

Scheme 2

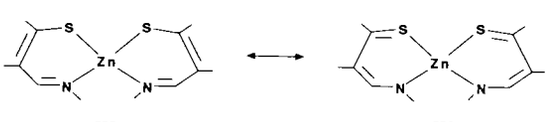

Scheme 3

concentration dependence for the kinetics was investigated in $CDCl_2CDCl_2$ (5.5–28 mmol dm^{-3} for complex **1**, 5–20 mmol dm^{-3} for **2**). Up to 115 °C for **2** and 124 °C for **1** no concentration dependence is observed. At higher temperatures the rate constants increase slightly with concentration indicating that second-order kinetics may be involved. Kinetic parameters (Table 6) were derived from plots of $\ln(k/T)$ *vs.* $1/T$ using equation (6) (see Experimental section) and assuming first-order

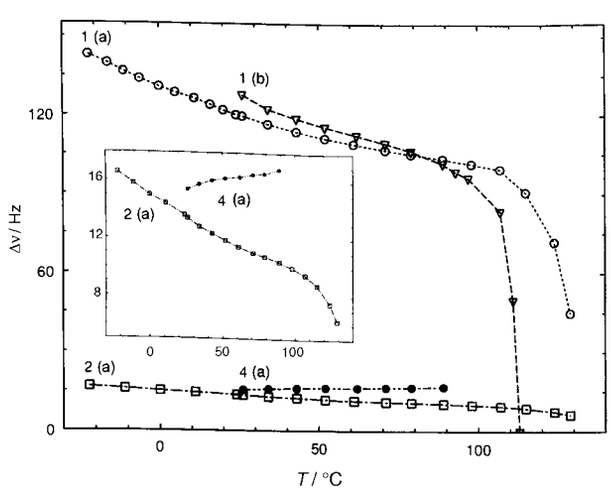

Fig. 6 Plots of $\Delta\nu$ *vs.* T for complexes **1**, **2** and **4** in (a) $CDCl_2CDCl_2$ and (b) $C_6D_5NO_2$

kinetics (see Fig. 7). Rate constants at 100 °C in $CDCl_2CDCl_2$ are 27.8 and 2.92 s^{-1} for complexes **1** and **2**, respectively, and 92.3 s^{-1} for **1** in $C_6D_5NO_2$.

Table 6 Activation parameters for the racemization process[a]

Complex	$\Delta H^{\ddagger}$/kJ mol^{-1}	$\Delta S^{\ddagger}$/J K^{-1} mol^{-1}	$\Delta G^{\ddagger}_{25}$/kJ mol^{-1}	Correlation coefficient[b]
1[c]	80.7 ± 6.1	−2.9 ± 17.2	81.6 ± 0.9	0.9974
1[d]	54.7 ± 5.8	−62.5 ± 16.2	73.3 ± 1.0	0.9936
2[c]	67.2 ± 6.4	−57.8 ± 17.1	84.4 ± 0.6	0.9963

[a] E.s.d.s were derived by the method described in ref. 13. [b] Of the Eyring plot. [c] Measured in $CDCl_2CDCl_2$. [d] Measured in $C_6D_5NO_2$.

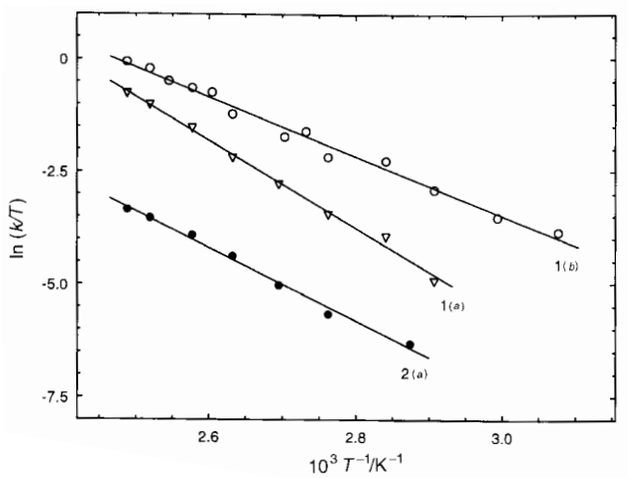

Fig. 7 Eyring plots (*a*) for complexes **1** and **2** in $CDCl_2CDCl_2$ and (*b*) for **1** in $C_6D_5NO_2$

The kinetic parameters for complex **1** in $CDCl_2CDCl_2$ are equal to those found for bis(β-aminothionato)zinc(II) complexes with isopropyl-substituted nitrogen donor atoms (measured in chlorobenzene).[12b] The replacement of Pr^i with 2,4,6-trimethylphenyl in a similar system strongly increases $\Delta H^{\ddagger}$ and $\Delta S^{\ddagger}$, on average for two indicator groups in the molecule of 96 kJ mol^{-1} and 62 J K mol^{-1}, respectively (measured in $CDCl_3$).[12a] A similar effect of the substituents on the nitrogen donor atoms in otherwise similar systems is seen here for complexes **1** and **2**.

As first-order kinetics are dominant in $CDCl_2CDCl_2$, the racemization mechanism is mainly intramolecular. Probably it is a twist mechanism through a planar transition state without rupture of M–L bonds, as most often proposed[3,6a,12b] for pseudo-tetrahedral Ni^{II} and Zn^{II}. The small numerical value of the activation entropy for complex **1** in $CDCl_2CDCl_2$ compared with that for **2** may be attributed to a *trans*-planar transition state for the former, a *cis*-planar and much more crowded transition state for the latter, in accordance with the crystal structures. Comparisons between **1** in $CDCl_2CDCl_2$ and $C_6D_5NO_2$ show that the kinetics are highly solvent dependent. The decrease in $\Delta H^{\ddagger}$ and $\Delta S^{\ddagger}$ in $C_6D_5NO_2$ may be due to a strong solvation of a planar activated complex, or to a change of mechanism. Concentration-dependence experiments were not performed in $C_6D_5NO_2$.

The absolute configuration for the zinc(II) complexes is much more stabilized than for the nickel(II) analogues described in separate papers (corresponding nickel complexes **1**,[3a] **2**,[3b] **4** and **5**[3c]). This is the usual trend:[6a,12b] $\Delta G^{\ddagger}$ at 25 °C is 47.2, 63.2 and 60.7 kJ mol^{-1} for the nickel equivalents **2**, **4** and **5**, respectively. The racemization rate for **1** (M = Ni) is too fast to be detected by ^{1}H NMR spectroscopy at −100 °C. The nickel(II) complexes were measured in CD_2Cl_2 (**1** and **2**) or in $CDCl_2CDCl_2$ (**4** and **5**). Comparisons between complexes **2** (M = Zn or Ni) show that the stability differences are due to $\Delta H^{\ddagger}$ (34.6 kJ mol^{-1} for Ni), as the change of metal ion leaves $\Delta S^{\ddagger}$ practically unaltered (−56.7 J K^{-1} mol^{-1} for Ni).[3b] The electronic argument for the configurational stability for the zinc(II) complexes is consistent with the assumption of a twist mechanism *via* a planar transition state, as tetrahedral and planar[14] co-ordination geometries are preferred by Zn^{II} and Ni^{II}, respectively.

Electronic spectra (see SUP 57186)

The evolution of the spectra of solutions of complexes **4** and **5** with time is shown in Fig. 8 together with the spectra of the pro-ligands H_2L. The spectra of the Schiff base *N*,*N*′-bis-5-sulfanylpyrazol-4-ylmethylene)ethane-1,2-diamine H_2L' (3-methyl-1-phenyl) [Fig. 8, inset (*a*)] and of the corresponding $(Bu^tS)_2$ derivative L″ are also shown. Temperature-dependent spectra were collected in the range 20–60 °C. Reversible line broadening and decreasing absorption coefficients with temperature are observed, characteristic of low-symmetry molecules.[15] A slow decomposition of the zinc(II) complexes with bidentate ligands, **1**–**3**, is observed for the dilute (μmol dm^{-3}) solutions used for the temperature- and time-dependent experiments. After 2 d in solution the spectrum of **3** is dominated by bands derived from the transitions of the pro-ligand. A development similar to that described for **4** and **5** below is observed for the more stable complexes **1** and **2** after 2 d in solution. The spectra of the pro-ligands are consistent with a shift of the tautomeric equilibrium (Scheme 2) to the left in solution. The $\pi \longrightarrow \pi^*$ transitions due to the thione form lose intensity, and bands at higher energies gain intensity with time. The slowness of the reaction is attributed to a geometrical change of the nitrogen donor atom from tetrahedral to planar. A similar shift of the tautomeric equilibrium has been observed also for (1*R*)-3-(hydroxymethylene)bornane-2-thione.[11c] The Schiff base derived from the condensation of this compound with ethane-1,2-diamine, however, maintains the thione form in solution.[11c] The spectra of freshly prepared samples of the zinc(II) chelates cannot be associated with the thioether/aldimine form observed for L″ rather with the resonance form of Scheme 3 also observed in the solid state for complexes **1** and **2**. A shift towards a thiolate-like mesomer with time, however, seems to take place. This is most clearly illustrated by the loss of intensity for the band at about 340 nm and by the simultaneous intensity increase for the bands at higher energies [see Fig. 8 for complex **5**, and inset (*b*) for complex **4**].

The two molecules of different symmetry observed for complex **5** in the NMR spectra cannot be distinguished in the UV spectrum, which is similar to that of the equally pyrazolyl-substituted complex **2** [Fig. 8, inset (*c*)].

Experimental

Materials

Chemicals for the preparations were reagent grade and commercially available, used as received. Solvents used for analytical purposes were spectroscopic grade. Acetonitrile used for cyclic voltammetry was boiled over phosphorus pentaoxide and distilled immediately before use.

Preparations

Schiff bases. The following general procedure was used to give the Schiff-base pro-ligands in acceptable yields (>50%).

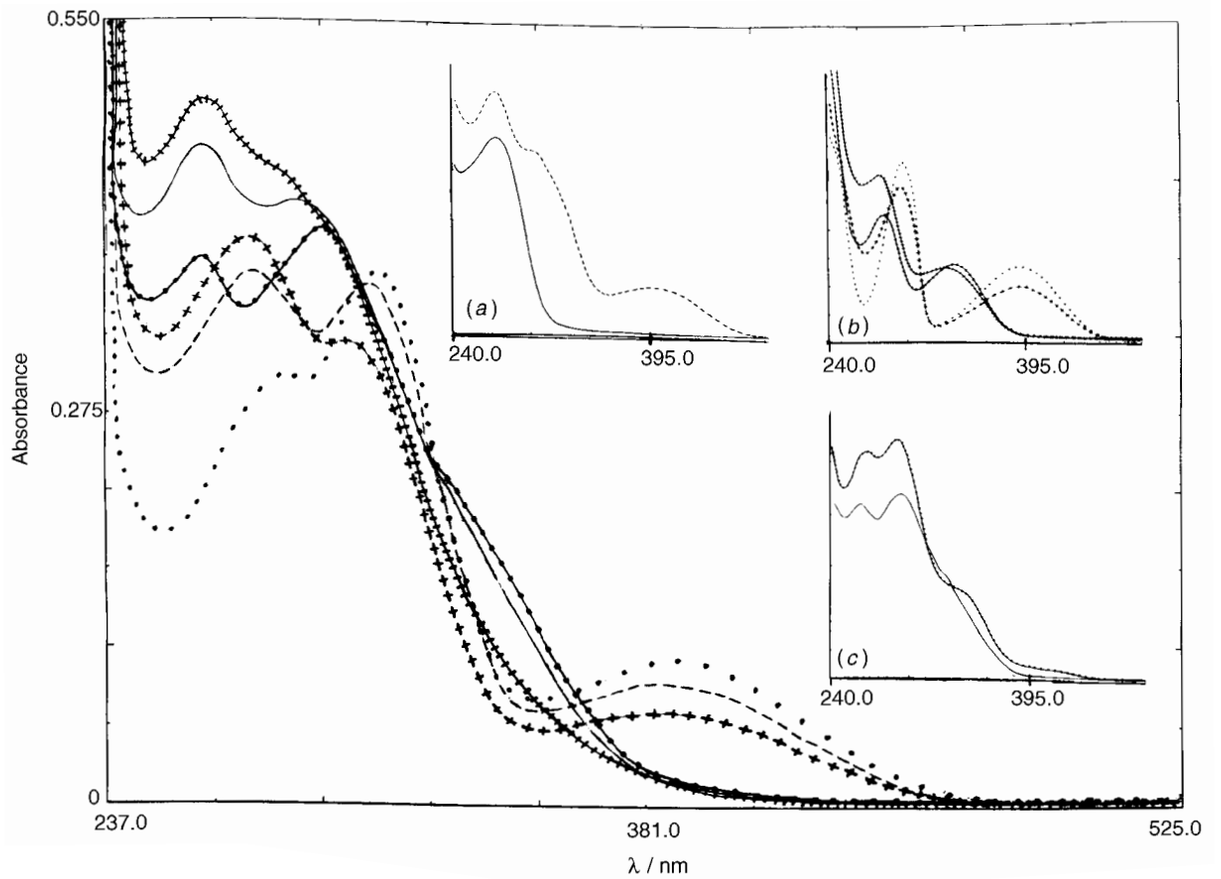

Fig. 8 Time-dependent electronic absorption spectra of complex **5** and its pro-ligand H_2L in $CHCl_3$ at 20 °C [shown for **4** in inset (*b*)]: fresh samples, complex (·–·–·–·), pro-ligand (···); after 2 d, complex (———), pro-ligand (– – –); after 4 d, complex (++++++), pro-ligand (+ + +). Spectra of L″ (———) (fresh sample) and of H_2L (– – –) (after a few days) are seen in inset (*a*), those of complexes **2** (·–·–·–·) and **5** (———) (fresh samples) in (*c*)

The appropriate *o*-chlorocarbaldehyde[16a] (6.8 mmol), $Na_2S·9H_2O$ (4.9 g, 20.4 mmol) and the appropriate amine (6.8 mmol) or diamine (3.4 mmol) were stirred at reflux temperature for 8–10 h in absolute EtOH (30–50 cm^3). Sodium chloride and some excess of Na_2S were filtered off. The excess of base in the filtrate was neutralized by formic acid, and N_2 was bubbled through the solution for about 0.5 h. The sodium formate was filtered off and the filtrate was concentrated. The yellow pro-ligand precipitated after 1–3 d, was filtered off and purified by preparative TLC, using MeOH–CH_2Cl_2 (1:9) as eluent. The SBu^t protected Schiff base (L″) and the analogous pro-ligand H_2L' were also prepared.[16b]

Complexes. The following general procedure was used. To a suspension of pro-ligand (0.2 mmol) in MeOH (3 cm^3) was added zinc(II) acetate dihydrate (complexes **1** and **2**, 0.1 mmol; **4** and **5**, 0.2 mmol) and NaOMe (3 mg Na in 0.5 cm^3 MeOH). The mixture was stirred at room temperature for 2 h. The white or pale yellow complex was filtered off and washed with MeOH on the filter. Analytical data are in Table 1. Complex **3** was prepared according to ref. 3(*b*).

Crystallography

Light yellow crystals of complex **1** were grown from MeCN–CH_2Cl_2 (about 4:1). Fast crystallization (in 4–5 d) in an open vessel resulted in the triclinic modification **1a** (space group $P\bar{1}$), whereas slow evaporation of the solvent (over more than 2 weeks) in a vial placed in a closed vessel containing paraffin resulted in the orthorhombic modification **1b** ($Pc2_1n$). Light yellow crystals of complex **2** were grown from EtOH–$CHCl_3$. The crystallographic experiments were performed at Colorado State University (**1a** and **2**) and at Odense University (**1b**) with Mo-Kα radiation (λ 0.710 73 Å). The cell constants were obtained by least-squares refinement from the setting angles of at least 25 reflections at the data collection temperatures (see below). The plotting program ORTEP II[17a] was used for the diagrams of **1**, the routine XP in SHELXTL[17b] for that of **2**. Details are given in Table 7.

Complex 1, modification 1a. Intensities were measured at −117 °C over 6 h using a Siemens SMART-CCD X-ray area-detector system. Data were corrected for Lorentz-polarization effects but not for absorption.[17b] Direct methods[17b] were used to solve the structure in the space group $P\bar{1}$. Full-matrix least-squares methods[17b] were employed to refine the coordinates and anisotropic displacement parameters for all non-hydrogen atoms. Hydrogen atoms were introduced at calculated positions [d(C–H) = 0.93 Å, $U_H = 1.2U_C$ (d 0.98 Å, $1.5U_C$ for methyl protons)].

Complex 1, modification 1b. Intensities were measured at room temperature using an Enraf-Nonius CAD-4F diffractometer. The intensity of one standard reflection was measured every 3 h and the decay corrected for. Data were corrected for Lorentz-polarization effects and for absorption.[17c] Relevant programs from XTAL 3.2[17d] were used to solve (in $Pc2_1n$ by direct methods) and to refine the structure (by full-matrix least-squares methods employing anisotropic thermal parameters for all non-hydrogen atoms). As refinement of the coordinates of an acetonitrile molecule resulted in a slightly bent structure (≈175°), only the thermal parameters were refined for this molecule. A few hydrogen atoms, not seen in the Δρ maps, were introduced at calculated positions [d(C–H) = 1.00 Å]. Hydrogen atoms were not refined. They were given a single isotropic thermal parameter ($U_H = 0.07$ Å^2). Weak reflections (4286

Table 7 Crystal data and details of data collection and structure refinement for complexes **1** and **2**[a]

	1a	**1b**	**2**
Formula	$C_{38}H_{36}N_6S_2Zn\cdot CH_3CN$	$C_{38}H_{36}N_6S_2Zn\cdot 0.5CH_3CN$	$C_{28}H_{32}S_2Zn$
M	747.295	726.769	582.101
Crystal system	Triclinic	Orthorhombic	Monoclinic
Space group	$P\bar{1}$	$Pc2_1n$	$C2$
a/Å	15.607(3)	8.377(2)	13.428(3)
b/Å	15.728(3)	23.18(1)	7.692(2)
c/Å	18.208(4)	36.94(1)	14.407(4)
α/°	94.22(3)	—	—
β/°	103.95(3)	—	103.98(2)
γ/°	118.16(3)	—	—
U/Å^3	3731.2(1)	7173 (4)	1444.0 (6)
Crystal size/mm	0.22 × 0.40 × 0.12	0.49 × 0.39 × 0.20	0.70 × 0.18 × 0.12
Developed forms	Irregular fragment	{100} {010} {001}	{001}{−201}{010}
D_c/g cm^{-3}	1.330	1.308	1.339
Z	4 (+4 CH_3CN)	8 (+4 CH_3CN)	2
μ/cm^{-1}	8.09	7.71	10.23
Transmission factors	—	0.737–0.859	0.809–0.881
θ limits/°	1–23	2–25	3–25
Octants collected[b]	$\pm h, \pm k, \pm l$	$+h, +k, +l$	$\pm h, +k, +l$
Standard reflections	—	2 0 11	600, 150, 006
Fall-off in intensity (%)	0	4.7	0
No. unique data	10 695[c]	6462	1383
No. observed data	9237[c]	4286	1346
[n in $I > n\sigma(I)$]	[2.0]	[2.5]	[2.0]
No. variables	916	864	178
$R1$[d]	0.056	0.080	0.032
$wR1$,[e] $wR2$[f]	0.125[f]	0.062[e]	0.081[f]
$\Delta\rho_{max}$, $\Delta\rho_{min}$/e Å^{-3}	0.79, −0.54	1.2,[g] −0.8	0.59, −0.52

[a] Data collection temperature: 25 °C (−117 °C for complex **1a**). [b] Followed by merging in the case of complex **1a**. [c] Merged data. [d] Refinement on F; $R1 = \Sigma(|F_o| - |F_c|)/\Sigma|F_o|$. [e] Refinement on F; $wR1 = [\Sigma w(|F_o| - |F_c|)^2/\Sigma w|F_o|^2]^{\frac{1}{2}}$ $w^{-1} = \sigma^2(F)$. [f] Refinement on F^2, $wR2 = \Sigma w(F_o^2 - F_c^2)^2/\Sigma w(F_o^2)^2$, $w^{-1} = \sigma^2F_o^2 + (0.0397P)^2 + 9.4963P$; $P = \frac{1}{3}(F_o^2 + 2F_c^2)$. [g] The highest residual peak is located 1.06 Å from Zn.

observed out of 6462 unique) resulted in a data set too limited for high quality of the large structure (864 variables), see Discussion above. Several attempts to solve and to refine the structure in the centrosymmetric space group *Pcmn* using direct methods or an integrated Patterson and direct-method procedure (the program PATSEE in XTAL 3.2)[17d] were unsuccessful (see Discussion above).

Complex 2. Intensities were measured at room temperature using a Siemens R3*m* diffractometer. No significant decomposition of the crystal occurred during the data collection. Data were corrected for Lorentz-polarization effects and for absorption.[17b] The structure was solved and refined in the space group *C*2 using the same methods as for complex **1**, modification **1a** (see above). The final value of the Flack absolute structure parameter,[17e,f] included as a free variable in the final full-matrix refinement, is 0.00(3) indicating that the correct enantiomorph was refined.

Atomic coordinates, thermal parameters, and bond lengths and angles have been deposited at the Cambridge Crystallographic Data Centre (CCDC). See Instructions for Authors, *J. Chem. Soc., Dalton Trans.*, 1997, Issue 1. Any request to the CCDC for this material should quote the full literature citation and the reference number 186/270.

Physical measurements

Proton and ^{13}C NMR spectra of the pro-ligands and complexes (5–28 mmol dm^{-3}) were obtained on Varian spectrometers (Gemini 200 and 300 and Unity 400 MHz). Methanol was used for temperature calibration at low temperature, ethylene glycol at high temperature. The uncertainty of the temperature is 1°. Assignments for pro-ligands and complexes were accomplished by comparisons between the systems and/or selective decoupling of single protons. Electrochemical data for complex **1** (1 mmol dm^{-3}) and its pro-ligand (2.5 mmol dm^{-3}) in MeCN were collected at room temperature under nitrogen by cyclic voltammetry. Conditions: micro-electrodes from BAS100 [platinum working and counter electrodes *vs.* an Ag–AgCl (water-based) reference electrode]; supporting electrolyte, NBu_4PF_6 (0.1 mol dm^{-3}); sweep rate, 0.200–0.650 V s^{-1}; external standard, ferrocene [$E_{\frac{1}{2}}(Fe^{II}–Fe^{III}) = 0.500$ V]. The electrolyte and the investigated compounds were dried in vacuum before use. The solvent with electrolyte was scanned before use to check the purity of the solvent. Electronic absorption spectra were obtained in $CHCl_3$ (concentrations of complexes and pro-ligands 10–30 μmol dm^{-3}) in a 1 cm quartz cuvette on a thermostatted Shimadzu UV-3100 apparatus. Electron-impact mass spectra were recorded on a Finnigan Mat SSQ710 or a Varian Mat 311A apparatus. Elemental analyses were performed at the H. C. Ørsted Institute, University of Copenhagen. The complexes were first dried in vacuum.

Determination of kinetic parameters for the racemization process

The temperature-dependent ^{1}H NMR spectra of exchanging chiral protons were used to determine the rate constants, $k(T)$, for the racemization process using equations (3)–(5), where T_c is

$$T \ll T_c\text{: } k(T) = \pi[\nu_{\frac{1}{2}}(T) - \nu_{\frac{1}{2}}^0] \quad (3)^{18a}$$

$$T \leqslant T_c\text{: } k(T) = 0.5\pi\{2[\Delta\nu^{02} - \Delta\nu^2(T)]\}^{\frac{1}{2}} \quad (4)^{18b}$$

$$T_c \leqslant T\text{: } k(T) = 0.5\pi\Delta\nu^0\{[\Delta\nu^0/\nu_{\frac{1}{2}}(T)]^2 - [\nu_{\frac{1}{2}}(T)/\Delta\nu^0]^2\}^{\frac{1}{2}} \quad (5)^{18c}$$

the coalescence temperature for the resonances of exchanging protons (indicator protons), $\nu_{\frac{1}{2}}^0$ and $\Delta\nu^0$ are the linewidth of and the chemical shift difference between the indicator protons, respectively, in the absence of exchange (they may be temperature dependent,[3,12b,13] as is the case for $\Delta\nu^0$ in this work) and $\nu_{\frac{1}{2}}(T)$ and $\Delta\nu(T)$ are the observed linewidth of and chemical shift difference between the indicator protons, respectively. The

activation parameters $\Delta H^{\ddagger}$ and $\Delta S^{\ddagger}$ were found from the plots of $\ln[k(T)/T]$ *vs.* $1/T$ using the Eyring equation (6), where k_B is the Bolzmann constant.

$$k(T) = T(k_B/h) \exp(\Delta S^{\ddagger}/R) \exp(-\Delta H^{\ddagger}/RT) \qquad (6)$$

Acknowledgements

We gratefully acknowledge Susie M. Miller, Colorado State University, for technical assistance with collection of data for complex **1a**, Inge Pedersen and Ole T. Sørensen, Odense University, for the mass spectra, and Brigitte Heinrich, Tamara Meinel and Jutta Ortwein, Leipzig University, for technical assistance with collection of NMR spectra.

References

1 (*a*) R. W. Hay, *Bioinorganic Chemistry*, Ellis Horwood, Chichester, 1987, pp. 12, 80, 85–99; (*b*) W. Kaim and B. Schwederski, *Bioinorganic Chemistry: Inorganic Elements in the Chemistry of Life*, eds. G. Meyer, A. Nakamura, G. Adachi and K. Poeppelmeier, Wiley, New York, 1994, ch. 12; (*c*) S. J. Lippard and J. M. Berg, *Principles of Bioinorganic Chemistry*, University Science Books, Mill Valley, CA, 1994, ch. 10.

2 H. Eklund, B. Nordström, E. Zeppezauer, G. Söderlund, I. Ohlsson, T. Boiwe, B.-O. Söderberg, O. Tapia, C. I. Bränden and Å. Åkeson, *J. Mol. Biol.*, 1976, **102**, 27.

3 (*a*) A. la Cour, M. Findeisen, K. Hansen, R. Hazell, L. Hennig and L. Petersen, unpublished work; (*b*) A. la Cour, B. Adhikhari, H. Toftlund and A. Hazell, *Inorg. Chim. Acta*, 1992, **202**, 145; (*c*) A. la Cour, M. Findeisen, C. E. Olesen and O. Simonsen, unpublished work.

4 G. Schneider, H. Eklund, E. Cedergren-Zeppezauer and M. Zeppezauer, *Proc. Natl. Acad. Sci. USA*, 1983, **80**, 5289.

5 (*a*) J. E. Huheey, *Inorganic Chemistry*, 3rd edn., Harper and Row, New York, 1983, pp. 258 and 259; (*b*) O. Simonsen, T. K. Hansen, J. Becher and S. Larsen, Poster presented at 14th Nordic Meeting of Structural Chemists, University of Helsinki, January 11–13, 1993; (*c*) C. T. Pedersen, *Sulfur Rep.*, 1980, **1**, 1; (*d*) C. T. Pedersen, *Phosphorus Sulfur Silicon Relat. Elem.*, 1991, **58**, 17.

6 (*a*) A. D. Garnowskii, A. L. Nivorozhkin and V. I. Minkin, *Coord. Chem. Rev.*, 1993, **126**, 1 and refs. therein; (*b*) M. J. E. Hewlins, *J. Chem. Soc., Dalton Trans.*, 1975, 429; (*c*) R. Cini, A. Cinquantini, P. Orioli and M. Sabat, *Inorg. Chim. Acta*, 1980, **41**, 151.

7 J. A. Kanters, A. L. Spek, R. Postma, G. C. van Stein and G. van Koten, *Acta Crystallogr., Sect. C*, 1983, **39**, 999; M. Dreher and H. Elias, *Z. Naturforsch., Teil B*, 1987, **42**, 707; H. Sakiyama, H. Okawa, N. Matsumoto and S. Kida, *J. Chem. Soc., Dalton Trans.*, 1990, 2935; E. Labisbal, J. Romero, A. de Blas, J. A. Garcia-Vazquez, M. L. Duran, A. Castineiras, A. Sousa and D. E. Fenton, *Polyhedron*, 1992, **11**, 53.

8 F. H. Allen, O. Kennard, D. G. Watson, L. Bremmer, A. G. Orpen and R. Taylor, *J. Chem. Soc., Perkin Trans., 2*, 1987, S1.

9 (*a*) H. Toftlund, A. L. Nivorozhkin, A. la Cour, B. Adhikhari, K. S. Murray, G. D. Fallon and L. E. Nivorozhkin, *Inorg. Chim. Acta*, 1995, **228**, 237 and refs. therein; (*b*) R. H. Holm and K. Swaminathan, *Inorg. Chem.*, 1962, **1**, 599.

10 (*a*) M. Kumar, R. O. Day, G. J. Colpas and M. J. Maroney, *J. Am. Chem. Soc.*, 1989, **111**, 5974; (*b*) M. Kumar, G. J. Colpas, R. O. Day and M. J. Maroney, *J. Am. Chem. Soc.*, 1989, **111**, 8323; (*c*) A. Böttcher, H. Elias, L. Müller and H. Paulus, *Angew. Chem., Int. Ed. Engl.*, 1992, **31**, 5; (*d*) T. Yamamura, M. Tadokoro, M. Hamaguchi and R. Kuroda, *Chem. Lett.*, 1989, 1481.

11 (*a*) R. Shabana, J. B. Rasmussen and S.-O. Lawessen, *Tetrahedron*, 1981, **37**, 1819; (*b*) L. Casella, M. Gulotti and A. Rockenbauer, *J. Chem. Soc., Dalton Trans.*, 1984, 1033; (*c*) L. Casella, M. Gulotti, R. Pagliarin and M. Sisti, *J. Chem. Soc., Dalton Trans.*, 1991, 2527.

12 (*a*) L. E. Konstantinovskii, R. Ya. Olekhnovitch, M. S. Korobov, L. E. Nivorozhkin and V. I. Minkin, *Polyhedron*, 1991, **10**, 771; (*b*) S. S. Eaton and R. H. Holm, *Inorg. Chem.*, 1971, **10**, 1446.

13 A. la Cour, M. Findeisen, A. Hazell, R. Hazell and G. Zdobinsky, following paper.

14 G. W. Everett, jun. and R. H. Holm, *Inorg. Chem.*, 1968, **7**, 776.

15 A. B. P. Lever, *Inorganic Electronic Spectroscopy*, 2nd edn., Elsevier, Amsterdam, 1984, pp. 191–193.

16 (*a*) J. Becher, P. H. Olsen, N. A. Knudsen and H. Toftlund, *Sulfur Lett.*, 1986, **4**, 175; (*b*) J. Becher, H. Toftlund, P. H. Olsen and H. Nissen, *Inorg. Chim. Acta*, 1985, **103**, 167.

17 (*a*) C. K. Johnson, ORTEP II, Report ORNL-5138, Oak Ridge National Laboratory, Oak Ridge, TN, 1976; (*b*) G. M. Sheldrick, SHELXTL, version 5, Siemens Analytical X-Ray Division, Madison, WI, 1994; (*c*) R. Norrestam and K. Nielsen, Technical University of Denmark, personal communication, 1982; (*d*) S. R. Hall, H. D. Flack and J. M. Stewart (Editors), *XTAL 3.2 Reference Manual*, Universities of Western Australia and Maryland, 1992; (*e*) H. D. Flack, *Acta Crystallogr., Sect. A*, 1983, **39**, 876; (*f*) G. Bernardinelli and H. D. Flack, *Acta Crystallogr., Sect. A*, 1985, **41**, 500.

18 (*a*) R. J. Abrahams, J. Fisher and P. Loftus, *Introduction to NMR Spectroscopy*, Wiley, New York, 1988, pp. 194–197; (*b*) S. Gutowsky and C. H. Holm, *J. Chem. Phys.*, 1956, **25**, 1228; (*c*) A. Allerhand, H. S. Gutowsky, J. Jonas and R. A. Meinzer, *J. Am. Chem. Soc.*, 1966, **88**, 3185.

Received 7*th May* 1996; *Paper* 6/03158G